Halo Nuclei with the Coulomb–Sturmian Basis

M. A. Caprio[a], P. Maris[b] and J. P. Vary[b]

[a] *Department of Physics, University of Notre Dame, Notre Dame, Indiana 46556, USA*
[b] *Department of Physics and Astronomy, Iowa State University, Ames, Iowa 50011, USA*

Abstract

The rapid falloff of the oscillator functions at large radius (Gaussian asymptotics) makes them poorly suited for the description of the asymptotic properties of the nuclear wave function, a problem which becomes particularly acute for halo nuclei. We consider an alternative basis for *ab initio* no-core configuration interaction (NCCI) calculations, built from Coulomb–Sturmian radial functions, allowing for realistic (exponential) radial falloff. NCCI calculations are carried out for the neutron-rich He isotopes, and estimates are made for the RMS radii of the proton and neutron distributions.

Keywords: *No-core configuration interaction; Coulomb–Sturmian basis; neutron halo; nuclear radii*

1 Introduction

The *ab initio* theoretical description of light nuclei is based on direct solution of the nuclear many-body problem given realistic nucleon-nucleon interactions. In no-core configuration interaction (NCCI) calculations [1, 2], the nuclear many-body problem is formulated as a matrix eigenproblem. The Hamiltonian is represented in terms of basis states which are antisymmetrized products of single-particle states for the full A-body system of nucleons, i. e., with no assumption of an inert core.

In practice, the nuclear many-body calculation must be carried out in a truncated space. The dimension of the problem grows combinatorially with the size of the included single-particle space and with the number of nucleons in the system. Computational restrictions therefore limit the extent to which converged results can be obtained, for energies or for other properties of the wave functions. Except for the very lightest systems ($A \lesssim 4$), convergence is generally beyond reach. Instead, we seek to approach convergence as closely as possible. Based on the still-unconverged calculations which are computationally feasible, we would then ideally be able to obtain a reliable estimate of the true values of observables which would be obtained in the full, untruncated space. Therefore, progress may be pursued both by seeking accelerated convergence, e. g., through the choice of basis, as considered here, and by developing means by which robust extrapolations can be made [3–7].

NCCI calculations have so far been based almost exclusively upon bases constructed from harmonic oscillator single-particle wave functions. The harmonic oscillator radial functions have the significant limitation that their asymptotic behavior is Gaussian, i. e., falling as $e^{-\alpha r^2}$ for large r. The actual asymptotics for nucleons bound by a finite-range force are instead expected to be exponential, i. e., falling as $e^{-\beta r}$.

The problem encountered in using an oscillator basis to describe a system with exponential asymptotics may be illustrated through the simple one-dimensional example of the Schrödinger equation with a Woods–Saxon potential. In Fig. 1, we see

Proceedings of International Conference 'Nuclear Theory in the Supercomputing Era — 2013' (NTSE-2013), Ames, IA, USA, May 13–17, 2013. Eds. A. M. Shirokov and A. I. Mazur. Pacific National University, Khabarovsk, Russia, 2014, p. 325.
http://www.ntse-2013.khb.ru/Proc/Caprio.pdf.

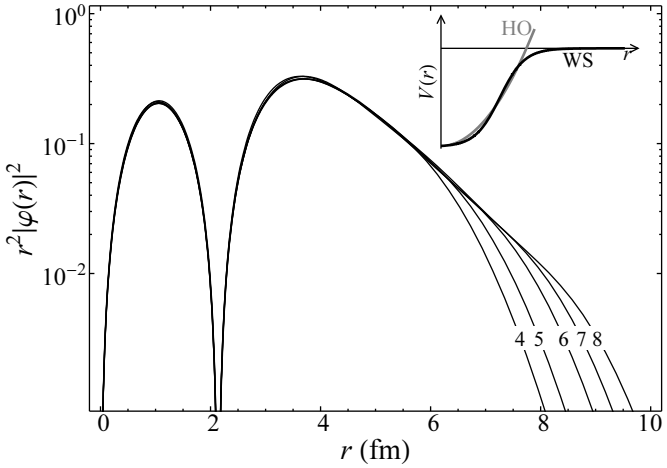

Figure 1: The calculated wavefunction obtained when a problem with exponential asymptotics — here, the Woods–Saxon problem is taken for illustration — is solved in a finite basis of oscillator functions. The radial probability density $r^2|\varphi(r)|^2$ is shown on a logarithmic scale, so that exponential asymptotics would appear as a straight line. The Woods–Saxon and oscillator potentials are shown in the inset. (Solutions are for the Woods–Saxon $1s_{1/2}$ function, with potential parameters appropriate to neutrons in ^{16}O [8], with maximal basis radial quantum numbers n as indicated.)

the results of solving for a particular eigenfunction in terms of successively larger bases of oscillator radial functions. In the classically forbidden region, where the potential is nearly flat, the tail of the wave function should be exponential. It should thus appear as a straight line on the logarithmic scale in Fig. 1. Inclusion of each additional basis function yields a small extension to the region in which the expected straight-line behavior is reproduced, but, for any finite number of oscillator functions, there is a radius beyond which the calculated tail is seen to sharply fall below the true asymptotics.

Observables which are sensitive to the large-radius asymptotic portions of the nuclear wave function therefore present a special challenge to convergence in NCCI calculations with a conventional oscillator basis. Such "long-range" observables include the RMS radius and $E2$ moments and transitions, since the r^2 dependence of the relevant operators in both cases preferentially weight the larger-r portions of the wave-function. The results for these observables in NCCI calculations are in general highly basis-dependent [9, 10].

Furthermore, a prominent feature in light nuclei is the emergence of halo structure [11], in which one or more loosely-bound nucleons surround a compact core, spending much of their time in the classically-forbidden region. A realistic treatment of the long-range properties of the wave function is essential for an accurate reproduction of the halo structure [12].

We are therefore motivated to consider alternative bases which might be better suited for expanding the nuclear wave function in its asymptotic region. The framework for carrying out NCCI calculations with a general radial basis is developed in Ref. [13]. We explore the use of the Coulomb–Sturmian functions [14–16], which form a complete set of square-integrable functions and have exponential asymptotics.

In the present work, we apply the Coulomb–Sturmian basis to NCCI calculations for the neutron halo nuclei ^{6,8}He — as well as to the baseline case ^{4}He, for which converged results can be obtained. We examine the possibility of extracting RMS radii for the proton and neutron distributions based on a relatively straightforward estimate, the "crossover point" [9,10], pending further development of more sophisticated

extrapolation schemes [5]. Motivated by the disparity between proton and neutron radial distributions in the neutron-rich halo nuclei, we also explore the use of proton-neutron asymmetric bases, with different length scales for the proton and neutron radial basis functions. The basis and methods are first reviewed (Section 2), after which the results for ^{4,6,8}He are discussed (Section 3).

2 Basis and methods

The harmonic oscillator basis functions, as used in conventional NCCI calculations, constitute a complete, discrete, orthogonal set of square-integrable functions and are given by $\Psi_{nlm}(b;\mathbf{r}) = R_{nl}(b;r)\,Y_{lm}(\hat{\mathbf{r}})/r$, with radial wave functions

$$R_{nl}(b;r) \propto (r/b)^{l+1} L_n^{l+1/2}\big[(r/b)^2\big] e^{-\frac{1}{2}(r/b)^2}, \tag{1}$$

where the L_n^α are generalized Laguerre polynomials, the Y_{lm} are spherical harmonics, n is the radial quantum number, l and m are the orbital angular momentum and its z-projection, and b is the oscillator length. The Coulomb–Sturmian functions likewise constitute a complete, discrete, orthogonal set of square-integrable functions, while also possessing exponential asymptotics more appropriate to the nuclear problem. They are given by $\Lambda_{nlm}(b;\mathbf{r}) = S_{nl}(b;r)\,Y_{lm}(\hat{\mathbf{r}})/r$, with radial wave functions

$$S_{nl}(b;r) \propto (2r/b)^{l+1} L_n^{2l+2}(2r/b) e^{-r/b}, \tag{2}$$

where b again represents a length scale. Further details may be found in Ref. [13]. Both sets of radial functions are shown in Fig. 2, for comparison.

For either basis, the single-particle basis states $|nljm\rangle$ are then defined by coupling of the orbital angular momentum with the spin, to give total angular momentum j, and the many-body basis is defined by taking antisymmetrized products of these single-particle states. Thus, the structure of the many-body calculation is independent of the details of the radial basis. The choice of radial basis only enters the calculation through the values of the Hamiltonian two-body matrix elements (or higher-body matrix elements, if present), which we must first generate as the input to the many-body calculation.

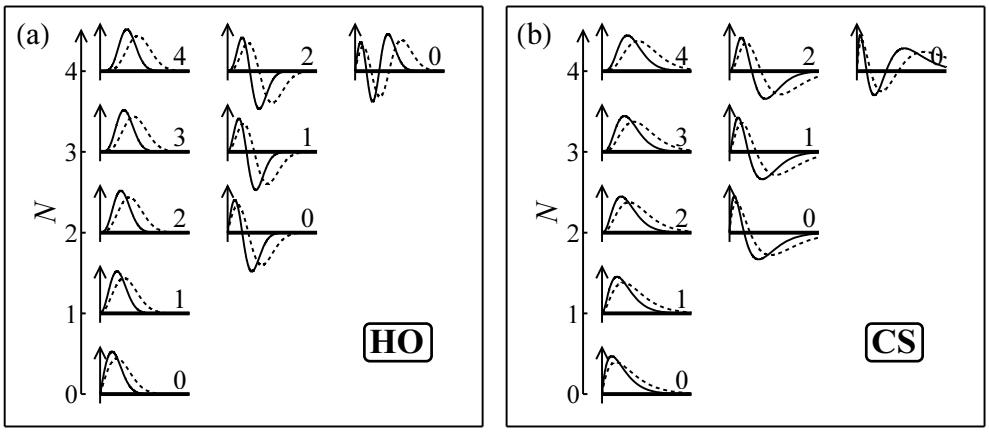

Figure 2: Radial functions (a) $R_{nl}(b;r)$ of the harmonic oscillator basis and (b) $S_{nl}(b_l;r)$ of the Coulomb–Sturmian basis, with b_l given by the node-matching prescription (see text). These functions are shown arranged according to the harmonic oscillator principal quantum number $N \equiv 2n + l$, and are labeled by l. The dotted curves show the same functions dilated outward by a factor of $\sqrt{2} \approx 1.414$.

The nuclear Hamiltonian for NCCI calculations has the form $H = T_{\rm rel} + V$, where $T_{\rm rel}$ is the Galilean-invariant, two-body relative kinetic energy operator, and V is the nucleon-nucleon interaction.[1] The relative kinetic energy decomposes into one-body and two-body terms as

$$T_{\rm rel} \equiv \frac{1}{4Am_N} \sum_{ij}{}' (\mathbf{p}_i - \mathbf{p}_j)^2 = \frac{1}{2Am_N} \left[(A-1) \sum_i \mathbf{p}_i^2 - \sum_{ij}{}' \mathbf{p}_i \cdot \mathbf{p}_j \right]. \tag{3}$$

Since the two-body term is separable, matrix elements of $T_{\rm rel}$ may be calculated in a straightforward fashion for any radial basis, in terms of one-dimensional radial integrals of the operators p and p^2 [13].

Calculation of the interaction two-body matrix elements becomes more involved if one moves to a general radial basis. The nucleon-nucleon interaction is defined in relative coordinates. The oscillator basis is special, in that matrix elements in a relative oscillator basis, consisting of functions $\Psi_{nl}(\mathbf{r}_1 - \mathbf{r}_2)$, can readily be transformed to the two-body oscillator basis, consisting of functions $\Psi_{n_1 l_1}(\mathbf{r}_1)\Psi_{n_2 l_2}(\mathbf{r}_2)$, by the Moshinsky transformation. We therefore still begin by carrying out the transformation to two-body matrix elements $\langle cd; J|V|ab; J\rangle$ with respect to the oscillator basis, and only then carry out a change of basis to the Coulomb–Sturmian basis in the two-body space, as [13]

$$\langle \bar{c}\bar{d}; J|V|\bar{a}\bar{b}; J\rangle = \sum_{abcd} \langle a|\bar{a}\rangle \langle b|\bar{b}\rangle \langle c|\bar{c}\rangle \langle d|\bar{d}\rangle \, \langle cd; J|V|ab; J\rangle, \tag{4}$$

where we label single-particle orbitals for the oscillator basis by unbarred symbols $a = (n_a l_a j_a)$ and those for the Coulomb–Sturmian basis by barred symbols $\bar{a} = (\bar{n}_a \bar{l}_a \bar{j}_a)$. The coefficients $\langle a|\bar{a}\rangle$ required for the transformation are obtained from straightforward one-dimensional overlaps of the harmonic oscillator and Coulomb–Sturmian radial functions, $\langle R_{nl}|S_{\bar{n}l}\rangle = \int_0^\infty dr\, R_{nl}(b_{\rm int}; r)\, S_{\bar{n}l}(b; r)$. The oscillator length $b_{\rm int}$ with respect to which the interaction two-body matrix elements are defined and the length scale b of the final Coulomb–Sturmian basis functions may in general be different. The change-of-basis transformation in (4) is, in practice, limited to a finite sum, e. g., with a shell cutoff $N_a, N_b, N_c, N_d \leq N_{\rm cut}$. The cutoff $N_{\rm cut}$ must be chosen high enough to insure that the results of the subsequent many-body calculation are cutoff-independent, which may in general depend upon the oscillator and Coulomb–Sturmian length parameters, interaction, nucleus, and observable at hand.

Any single particle basis, including (1) or (2), has a free length scale b. For the oscillator basis, this is traditionally quoted as the oscillator energy $\hbar\Omega$, where

$$b(\hbar\Omega) = \frac{(\hbar c)}{[(m_N c^2)(\hbar\Omega)]^{1/2}}. \tag{5}$$

In deference to the convention of presenting NCCI results as a function of the basis "$\hbar\Omega$", we nominally carry over this relation to define an $\hbar\Omega$ parameter for general radial bases, although $\hbar\Omega$ no longer has any direct physical meaning as an energy scale. Regardless, the inverse square-root dependence remains, so that a factor of two change in $\hbar\Omega$ describes a factor of $\sqrt{2}$ change in radial scale, as illustrated for both harmonic oscillator and Coulomb–Sturmian bases by the dotted curves in Fig. 2.

Furthermore, there is much additional freedom in the basis, since the many-body basis states (antisymmetrized product states) constructed from a single-particle basis are orthonormal so long as the single-particle states are orthonormal. Orthogonality for single-particle states of different l or j follows entirely from the angular and

[1] A Lawson term proportional the number $N_{\rm c.m.}$ of center-of-mass oscillator quanta can also be included, to shift center-of-mass excitations out of the low-lying spectrum, but it is not essential for the ground-state properties considered here. The implications of center-of-mass dynamics for general bases are addressed in Ref. [13].

spin parts of the wave function. Only orthogonality *within* the space of a given l and j follows from the radial functions, e. g., for the Coulomb–Sturmian functions, $\langle n'l'j'|nlj\rangle = \left[\int dr\, S_{n'l}(b;r)\, S_{nl}(b;r)\right] \delta_{l'l}\delta_{j'j}$. We are therefore free to choose b independently, firstly, for each l space (or j space), as b_l (or b_{lj}), and, secondly, for protons and neutrons, as b_p and b_n.

The first observation raises the possibility, still to be explored, of obtaining significant improvements in the efficacy of the basis by optimizing the l-dependence of the length parameter. In Ref. [13], the radial scale of the Coulomb–Sturmian functions, for each l, was fixed by matching the first node of the $n = 1$ Coulomb–Sturmian function to the first node of the $n = 1$ oscillator function, at that l, yielding the prescription $b_l = [2/(2l+3)]^{1/2} b(\hbar\Omega)$ [13].

The second observation raises the possibility of proton-neutron asymmetric length scales, which might be advantageous for nuclei with significant disparities between the proton and neutron distributions, in particular, halo nuclei. Therefore, in the present work, we adopt

$$b_{l,p} = \sqrt{\frac{2}{2l+3}}\, b(\hbar\Omega), \qquad b_{l,n} = \beta \sqrt{\frac{2}{2l+3}}\, b(\hbar\Omega), \tag{6}$$

where β sets an overall relative scale b_n/b_p. For example, if the solid and dotted curves in Fig. 2(b) are taken to represent the proton and neutron radial functions, respectively, then the figure illustrates the case in which $b_n/b_p = \sqrt{2} \approx 1.414$.

3 Results for the He isotopes

We carry out calculations for the isotopes ^{4,6,8}He using both the harmonic oscillator and Coulomb–Sturmian bases. These calculations are based on the JISP16 nucleon-nucleon interaction [17], plus Coulomb interaction. The bare interaction is used, i. e., without renormalization. The proton-neutron M-scheme code MFDn [18, 19] is employed for the many-body calculations. Results are calculated with basis truncations up to $N_{\max} = 14$ for ^{4}He, $N_{\max} = 12$ for ^{6}He, and $N_{\max} = 10$ for ^{8}He.[2]

The last neutrons in ^{6}He and ^{8}He are only weakly bound, with two-neutron separation energies of 0.97 MeV and 2.14 MeV, respectively. These isotopes are interpreted as consisting of neutron halos surrounding an α core [11]. The basic observables indicating halo properties are the RMS radii of the proton and neutron distributions, r_p and r_n, respectively.[3] Moving from ^{4}He to ^{6}He, r_p increases by ∼32%. This may be understood as resulting from the recoil of the α core against the halo neutrons, and potentially core polarization, as well. In turn, r_n is larger than r_p by ∼42%, reflecting the extended halo neutron distribution. The radii for ^{8}He are comparable to those for ^{6}He.

We first consider calculations for ^{4}He as a baseline. Results are shown over two doublings in $\hbar\Omega$, i. e., representing a doubling in basis length scale, in Fig. 3. Energy convergence is reached for the harmonic oscillator basis, as evidenced by approximate $N_{\max}$ and $\hbar\Omega$ independence of the higher $N_{\max}$ results over a range of $\hbar\Omega$ values, in Fig. 3(a, b). Convergence is obtained at the ∼10 keV level by $N_{\max} = 14$. The

[2]The harmonic oscillator many-body basis is normally truncated according to the $N_{\max}$ scheme, based on the total number of oscillator quanta. That is, the many-body basis states are characterized by a total number of oscillator quanta $N_{\rm tot} \equiv \sum_i N_i$, where $N_i \equiv 2n_i + l_i$. If $N_{\rm tot}$ is written as $N_{\rm tot} = N_0 + N_{\rm ex}$, where N_0 in the lowest Pauli-allowed number of quanta, then the basis is subject to the restriction $N_{\rm ex} \le N_{\max}$. We formally carry this truncation over to the Coulomb–Sturmian basis, although $N \equiv 2n + l$ no longer has significance as an oscillator principal quantum number.

[3]Specifically, r_p and r_n are the RMS radii of the point-proton and point-neutron distributions, measured relative to the center of mass. See Ref. [20] for definitions, and Ref. [13] for evaluation of the two-body relative RMS radius observable with a general radial basis. From the analysis of experimental charge and matter radii in Ref. [11], ^{4}He has $r_p = 1.457(10)$ fm ($\approx r_n$), ^{6}He has $r_p = 1.925(12)$ fm and $r_n = 2.74(7)$ fm, and ^{8}He has $r_p = 1.807(28)$ fm and $r_n = 2.72(4)$ fm.

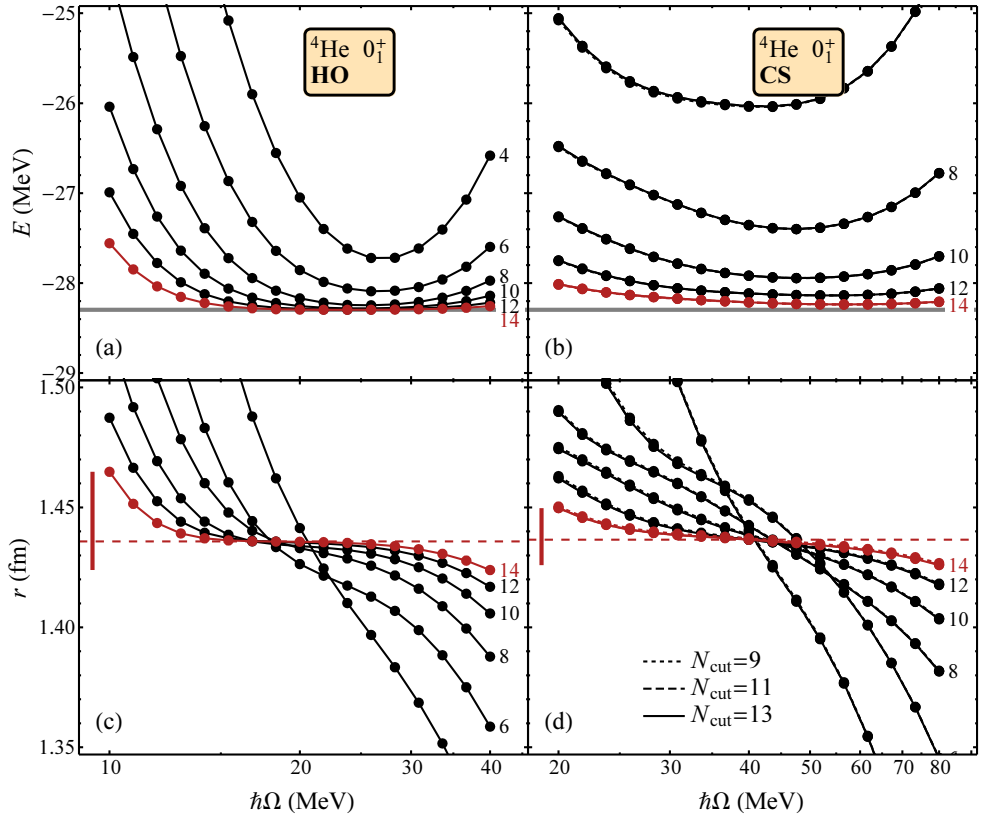

Figure 3: The calculated ^{4}He ground state energy (top) and RMS point-proton radius r_p (bottom), using the conventional oscillator (left) and Coulomb–Sturmian (right) bases. These are shown as functions of the basis $\hbar\Omega$ parameter, for $N_{\rm max} = 4$ to 14 (as labeled), and for transformation cutoffs $N_{\rm cut} = 9$, 11, and 13 (Coulomb–Sturmian basis only, indicated by dashing, curves nearly indistinguishable). The converged energy is indicated by the horizontal line (at top), the crossover radii by dashed horizontal lines (at bottom), and the spread in radius values by vertical bars (again at bottom).

binding energies for ^{4}He computed with the Coulomb–Sturmian basis lag significantly behind those obtained with the oscillator basis, by about two steps in $N_{\rm max}$. This should perhaps not be surprising, given that ^{4}He is tightly bound, and the structure can thus be expected to be driven by short-range correlations rather than asymptotic properties. Incidentally, it may be seen from Fig. 3(b, d) that stability with respect to the cutoff in the change-of-basis transformation (4) has been obtained — calculations with $N_{\rm cut} = 9$, 11, and 13 are virtually indistinguishable (the transformation has been carried out from oscillator basis interaction matrix elements at $\hbar\Omega_{\rm int} = 40\,$MeV).

Convergence of the computed RMS radii, for both the oscillator and Coulomb–Sturmian bases, is again indicated by approximate $N_{\rm max}$ and $\hbar\Omega$ independence over a range of $\hbar\Omega$ values, which appears as a shoulder in the curves of Fig. 3(c, d). The $\hbar\Omega$ dependence for the Coulomb–Sturmian calculations appears to be moderately shallower, over the range (two doublings) of $\hbar\Omega$ shown, than for the harmonic oscillator calculations [see vertical bars in Fig. 3(c, d)].

It was proposed in Refs. [9, 10] that the radius can be estimated — even before convergence is well-developed — by the crossover point between the curves obtained for successive $N_{\rm max}$ values. This is an admittedly *ad hoc* prescription, rather than a theoretically motivated extrapolation. However, we can test it — for both oscillator

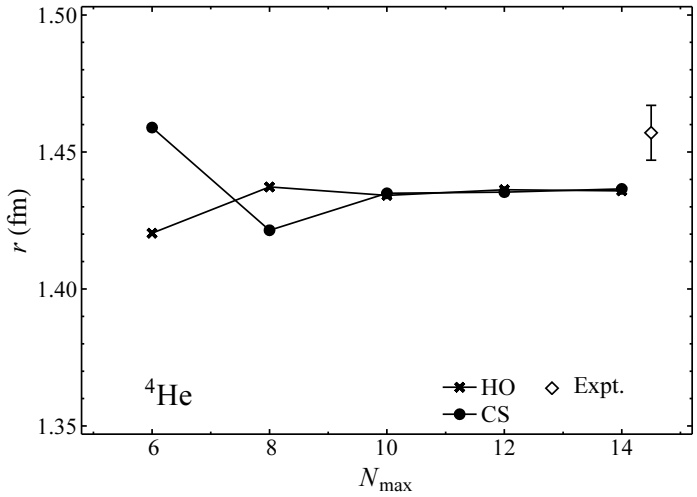

Figure 4: The ^{4}He ground state RMS point-proton radius r_p, as estimated from the crossover point (see text), calculated for the harmonic oscillator and Coulomb–Sturmian bases. The experimental value is from Ref. [11].

and Coulomb–Sturmian bases — in this case of ^{4}He, where the final converged value is known. The crossover radii are shown as a function of $N_{\max}$, for both bases, in Fig. 4. The curves used in deducing these crossovers are computed by cubic interpolation of the calculated data points at different $\hbar\Omega$. The crossovers already serve to estimate the final converged value to within $\sim$0.05 fm at $N_{\max} = 6$. It may be noted, from Fig. 4, that the converged radius obtained with the JISP16 interaction agrees with experiment to within $\sim$0.03 fm.

Let us now consider the calculations for the halo nuclei ^{6,8}He. The computed ground state energies, proton radii, and neutron radii are shown in Figs. 5 and 7. Results are included (at right in each figure) for a Coulomb–Sturmian basis with proton-neutron asymmetric length scales in the ratio $b_n/b_p = 1.414$, which is comparable to the ratio r_n/r_p of neutron and proton distribution radii for these nuclei. Energy convergence in the Coulomb–Sturmian basis lags that of the harmonic oscillator basis, but less dramatically than seen above for ^{4}He. A basic three-point exponential extrapolation of the energy with respect to $N_{\max}$, at each $\hbar\Omega$ value, is indicated by the dashed curves in Figs. 5 and 7. The extrapolated energy is remarkably $\hbar\Omega$-independent in the $b_n/b_p = 1.414$ calculations, still with some $N_{\max}$ dependence. It appears to be approximately consistent with the harmonic oscillator extrapolations as well. However, such extrapolations must be viewed with caution, as both theoretical arguments and empirical studies suggest that other functional forms may be more appropriate, over at least portions of the $\hbar\Omega$ range [4–6].

Comparing the results for radii obtained with the various bases, for ^{6,8}He, we see that the Coulomb–Sturmian results (for either $b_n/b_p = 1$ or $b_n/b_p = 1.414$) again have a moderately shallower $\hbar\Omega$ dependence than obtained with the harmonic oscillator basis. Well-defined and stable crossover points are visible in Figs. 5 and 7, especially for the $b_n/b_p = 1.414$ calculations (at right). The extracted crossover radii are shown, as functions of $N_{\max}$, in Figs. 6 and 8. The radii obtained for the Coulomb–Sturmian calculations with different ratios of neutron and proton length scales ($b_n/b_p = 1$, 1.189, and 1.414) track each other closely from $N_{\max} \approx 8$ onward, agreeing with each other to within $\sim$0.1 fm. For r_p, the values are stable with respect to $N_{\max}$ and agree with the values obtained from the harmonic oscillator basis crossover as well. For r_n, it appears that the values might be drifting systematically with $N_{\max}$, although they do remain within an $\sim$0.2 fm range from $N_{\max} = 6$ onward. (The

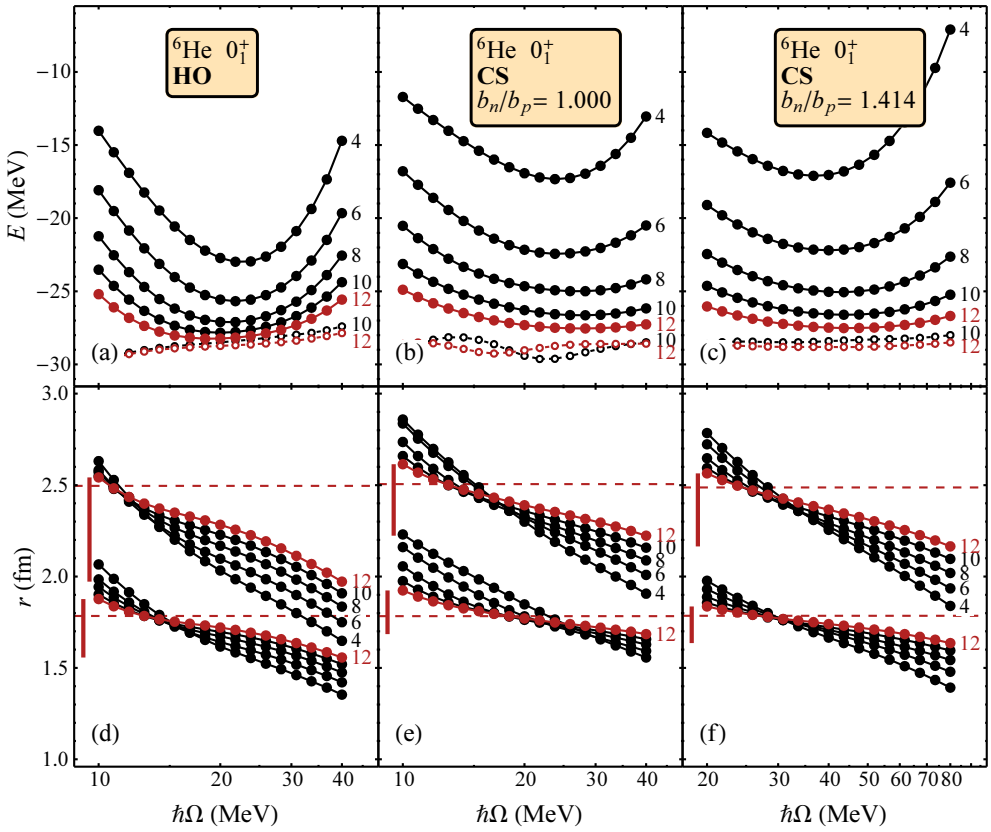

Figure 5: The calculated ^{6}He ground state energy (top) and RMS point-proton radius r_p and point-neutron radius r_n (bottom), using the conventional oscillator basis (left), Coulomb–Sturmian basis (center), and Coulomb–Sturmian basis with $b_n/b_p = 1.414$ (right). Exponentially extrapolated energies are indicated by dashed curves (at top), and crossover radii by dashed horizontal lines (at bottom).

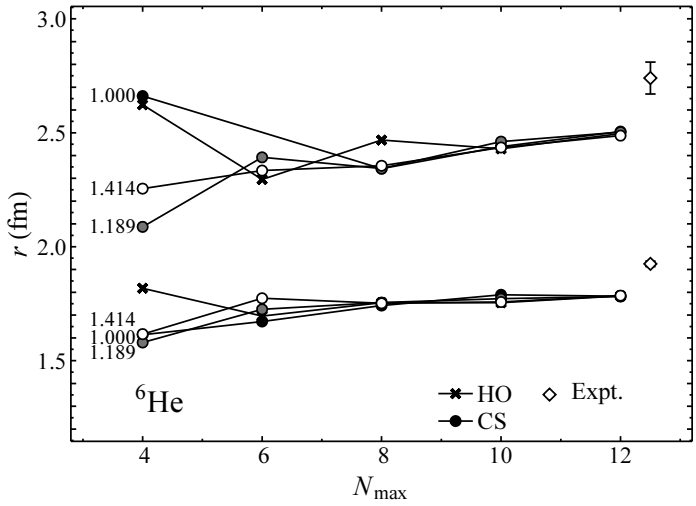

Figure 6: The ^{6}He ground state RMS point-proton radius r_p (lower curves) and point-neutron radius r_n (upper curves), as estimated from the crossover point (see text), calculated for the harmonic oscillator basis and for Coulomb–Sturmian bases with $b_n/b_p = 1$, 1.189, and 1.414 (as indicated). Experimental values are from Ref. [11].

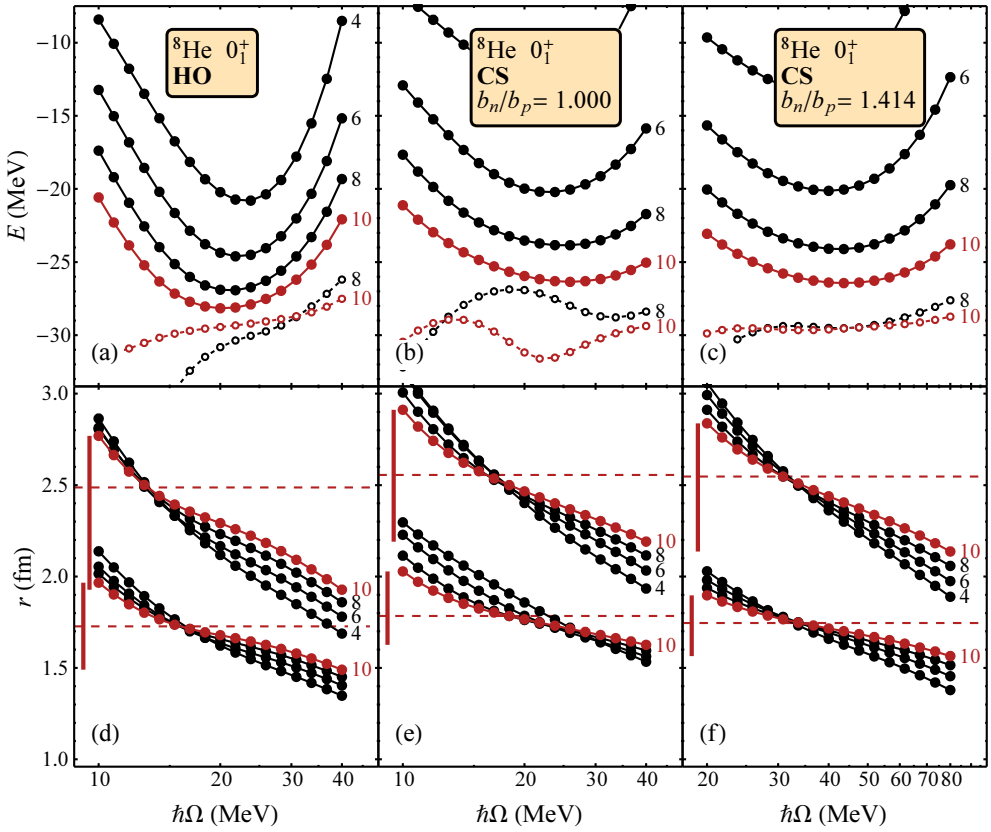

Figure 7: The calculated ^{8}He ground state energy (top) and RMS point-proton radius r_p and point-neutron radius r_n (bottom), using the conventional oscillator basis (left), Coulomb–Sturmian basis (center), and Coulomb–Sturmian basis with $b_n/b_p = 1.414$ (right). Exponentially extrapolated energies are indicated by dashed curves (at top), and crossover radii by dashed horizontal lines (at bottom).

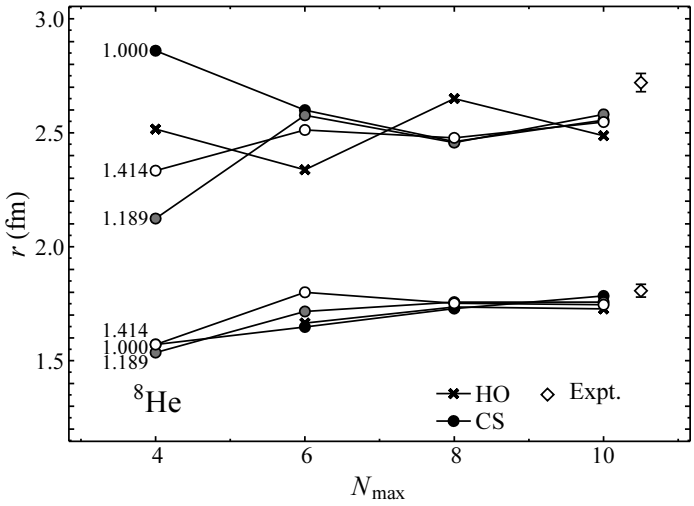

Figure 8: The ^{8}He ground state RMS point-proton radius r_p (lower curves) and point-neutron radius r_n (upper curves), as estimated from the crossover point (see text), calculated for the harmonic oscillator basis and for Coulomb–Sturmian bases with $b_n/b_p = 1$, 1.189, and 1.414 (as indicated). Experimental values are from Ref. [11].

crossover radii obtained from the harmonic oscillator calculations are fluctuating over a wider range.) Therefore, it is not possible to give a definitive value, but an estimate of $r_n \approx 2.5$–$2.6\,\mathrm{fm}$ can reasonably be made, for both ^{6,8}He.

Thus, *ab initio* NCCI calculations for ^{6,8}He with the JISP16 interaction, using both conventional and Coulomb–Sturmian bases, yield consistent estimates of the RMS point-proton and point-neutron radii, when these are extracted by the crossover prescription. The results qualitatively reproduce the trend in proton and neutron radii across the He isotopes, while quantitatively suggesting that the JISP16 interaction may yield radii which are smaller than experimentally observed, by as much as $\sim$0.2–0.3 fm for the ^{6,8}He neutron radii.

Acknowledgements

We thank S. Quaglioni, S. Bacca, and M. Brodeur for valuable discussions and A. E. McCoy for comments on the manuscript. This work was supported by the Research Corporation for Science Advancement through the Cottrell Scholar program, by the US Department of Energy under Grants No. DE-FG02-95ER-40934, DESC0008485 (SciDAC/NUCLEI), and DE-FG02-87ER40371, and by the US National Science Foundation under Grant No. 0904782. Computational resources were provided by the National Energy Research Supercomputer Center (NERSC), which is supported by the Office of Science of the U.S. Department of Energy under Contract No. DE-AC02-05CH11231.

References

[1] P. Navrátil, J. P. Vary and B. R. Barrett, Phys. Rev. Lett. **84**, 5728 (2000); Phys. Rev. C **62**, 054311 (2000).

[2] B. R. Barrett, P. Navrátil and J. P. Vary, Progr. Part. Nucl. Phys. **69**, 131 (2013).

[3] P. Maris, J. P. Vary and A. M. Shirokov, Phys. Rev. C **79**, 014308 (2009).

[4] S. A. Coon, M. I. Avetian, M. K. G. Kruse, U. van Kolck, P. Maris and J. P. Vary, Phys. Rev. C **86**, 054002 (2012).

[5] R. J. Furnstahl, G. Hagen and T. Papenbrock, Phys. Rev. C **86**, 031301 (2012).

[6] S. N. More, A. Ekstrom, R. J. Furnstahl, G. Hagen and T. Papenbrock, Phys. Rev. C **87**, 044326 (2013).

[7] E. D. Jurgenson, P. Maris, R. J. Furnstahl, P. Navratil, W. E. Ormand and J. P. Vary, Phys. Rev. C **87**, 054312 (2013).

[8] J. Suhonen, *From nucleons to nucleus*. Springer-Verlag, Berlin, 2007.

[9] S. K. Bogner, R. J. Furnstahl, P. Maris, R. J. Perry, A. Schwenk and J. Vary, Nucl. Phys. A **801**, 21 (2008).

[10] C. Cockrell, J. P. Vary and P. Maris, Phys. Rev. C **86**, 034325 (2012).

[11] I. Tanihata, H. Savajols and R. Kanungo, Progr. Part. Nucl. Phys. **68**, 215 (2013).

[12] S. Quaglioni and P. Navrátil, Phys. Rev. C **79**, 044606 (2009).

[13] M. A. Caprio, P. Maris and J. P. Vary, Phys. Rev. C **86**, 034312 (2012).

[14] M. Rotenberg, Ann. Phys. (NY) **19**, 262 (1962).

[15] E. J. Weniger, J. Math. Phys. **26**, 276 (1985).

[16] B. D. Keister and W. N. Polyzou, J. Comput. Phys. **134**, 231 (1997).

[17] A. M. Shirokov, J. P. Vary, A. I. Mazur and T. A. Weber, Phys. Lett. B **644**, 33 (2007).

[18] P. Maris, M. Sosonkina, J. P. Vary, E. Ng and C. Yang, Proc. Comput. Sci. **1**, 97 (2010).

[19] H. M. Aktulga, C. Yang, E. G. Ng, P. Maris and J. P. Vary, Concurrency Computat.: Pract. Exper. (2013), DOI: 10.1002/cpe.3129.

[20] S. Bacca, N. Barnea and A. Schwenk, Phys. Rev. C **86**, 034321 (2012).